An analysis of disentangled spectra of the double-lined eclipsing binary AR Aurigae by means of spectrum synthesis

Abundance determination of chosen chemical elements

J. Zverko[1], J. Žižňovský[1] and V.L. Khokhlova[2]

[1] *Astronomical Institute of the Slovak Academy of Sciences 059 60 Tatranská Lomnica, The Slovak Republic*

[2] *Institute of Astronomy, Russian Academy of Sciences, Pyatnitskaya 48, 109 017 Moscow, Russia*

Received: February 13, 1997

Abstract. Photographic spectra of AR Aur, the spectroscopic double-lined (SB2) binary with chemically peculiar components, were disentangled using the KOREL code and abundances of chosen chemical elments were determined by means of spectrum synthesis. In the A - component, for $T_{\rm eff} = 10\,950$ K and $\log g = 4.33$, Mn, Zr, Ba, Pt and Hg were found overabundant by factors of 12, 21, 13, 1350 and $2.2\,10^6$, respectively. In the B - component, for $T_{\rm eff} = 10\,350$ K and $\log g = 4.20$, Mn, Ba and Pt were found overabundant by factors of 5, 170 and 300, respectively. The overabundances derived differ from the previous ones, except for Mn in the B - component.

Key words: stars – binaries – chemically peculiar – abundance determination

1. Introduction

The double-lined spectroscopic eclipsing binary AR Aurigae (17 Aur, HR 1728 HD 34 364) has been well studied by many authors from various aspects. First, Wolff & Wolff (1976) and Wolff & Preston (1978) classified the primary component as an Hg and HgMn-star, respectively. Takeda et al.(1979) reported an occurrence of the HgII line $\lambda\,398.4$ nm in the spectrum near the phase of secondary minimum. Chochol et al.(1988) discovered a third body in the system, and Nordström & Johansen (1994) studied and derived the parameters of the multiple system in detail. Khokhlova et al.(1995) (hereinafter referred as paper KZZG) determined elemental abundances in both components by means of differential analysis relatively to other well studied HgMn CP-stars. Being an eclipsing double-lined binary with chemically peculiar components, AR Aurigae

also offers a unique possibility of studying the evolutionary aspects of the chemical peculiarity phenomenon. A more detailed history of the investigation of the binary can be found in the papers cited above and in references given therein.

In this study we apply a new code KOREL (Hadrava 1995, 1996) in order to disentangle the same high-dispersion photographic spectra that were used in KZZG. While analysing composite spectra, one encounters problems such as mutual blendig of lines originating in the individual binary components, decomposed spectra enable simpler procedures to be used for single stars. Thus, in addition to the line list given in the previous work, we were able to identify lines of MnI in spectra of both components, as well as a line of platinum in the spectrum of the secondary component. We pay attention, with respect to the results of previous analyses, especially to mercury and to the other elements featuring chemical peculiarity. The abundances of the elements were determined by means of spectrum synthesis.

2. Disentangling spectra and abundance determination

The method and the use of the KOREL code is described in Hadrava (1995, 1996). In the result it yields decomposed spectra of each component, as well as a simultaneous solution of orbital elements. We have used the PC-version of the code.

The digitized records of photographic spectrograms used were the same as in KZZG. The spectrograms were obtained by one of the authors (V.L.Khokhlova) and W.Wehlau with the 6-m BTA reflector of the Special Astrophysical Observatory in November 1986. The spectrograms were reduced on PDS microdensitometer at the Greenwich Observatory by one of the authors (VLK). The original plate factor was 0.17 nm mm^{-1}, and the records yield 200 readings per nm. The records covering wavelengths from 391 to 463 nm were split into 47 approximately 2 nm long and mutually overlapping sections. As we had no possibility of treating long sections of spectra, and as the KOREL needs continuum points at each end of the section being disentangled, we had to partly rectify the spectra sometimes relatively to the wings of hydrogen lines. The decomposed sections of the spectra of the individual components were then fitted with a synthetic spectrum computed by the SYNSPEC code (Hubený 1987, Zboril 1989).

We used the same values of the effective temperature and surface gravity as in KZZG, i.e. $T_{\mathrm{eff}} = 10\,950$ K and $\log g = 4.33$ for the primary (A) component and $T_{\mathrm{eff}} = 10\,350$ K and $\log g = 4.20$ for the secondary (B) component. These values were derived by Nordström & Johansen (1994) who carefully evaluated the previous determination from spectrophotometry, Strömgren photometry and light-curve solution. The rms erros given by the authors are $\pm$300K and $\pm$0.025 for temperature and $\log g$, respectively. The microturbulent velocity parameter $\xi_{\mathrm{turb}} = 0.5\,\mathrm{km\ s}^{-1}$ was also taken from the KZZG. The atmosphere models were

interpolated to these values from the grid of Kurucz's ATLAS9 models (Kurucz 1993). Unless stated otherwise, the $\log gf$ values are according to Kurucz (1993). The system and components physical parameters are summarized in Table 1.

Table 1. The system and component parameters of AR Aur according to Nordström & Johansen (1994)

Parameter	Primary	Secondary
M	$2.48\,M_\odot$	$2.29\,M_\odot$
R	$1.78\,R_\odot$	$1.82\,R_\odot$
$T_{\rm eff}$	10950 K	10350 K
$\log g$	4.33	4.28
$v \sin i$ (comp)	$21.8\,{\rm km\,s^{-1}}$	$22.3\,{\rm km\,s^{-1}}$
$i_{\rm orb}$	88.56°	
Ephemeris	$JD_{\rm Prim.min} = 2\,439\,156.7636+$	
	$4.1346905\,{\rm E}$	

The projected rotational velocity, $v \sin i = 22\,{\rm km\ s^{-1}}$, was adapted for the fitting procedure. The half-width of the instrumental profile of the spectrograph used (Romanyuk 1996) corresponds to 13 km s^{-1}. A synthetic spectrum was computed repeatedly varying the abundance of the element concerned until an accepetable agreement with the observed, within S/N $\approx$ 50, was reached.

3. Results

Starting with the abundances of the chemical elements given in KZZG, we first derived the abundances of iron, titanium and chromium as the elements with the most abundant lines, often occurring in blends with the lines of other elements in the spectrum. The results are summarized in Table 2.

Table 2. Abundances of elements relative to hydrogen

Element	Primary	KZZG (A)	Secondary	KZZH (B)	Normal
Ti	$5.03\ 10^{-7}$	$7.94\ 10^{-7}$	$2.04\ 10^{-7}$	$4.57\ 10^{-7}$	$8.91\ 10^{-8}$
Cr	$3.25\ 10^{-6}$	$2.04\ 10^{-6}$	$1.92\ 10^{-6}$	$2.04\ 10^{-6}$	$4.27\ 10^{-7}$
Mn	$2.74\ 10^{-6}$	$9.12\ 10^{-6}$	$1.21\ 10^{-6}$	$1.58\ 10^{-6}$	$2.24\ 10^{-7}$
FeI	$1.90\ 10^{-4}$	$8.32\ 10^{-5}$	$6.25\ 10^{-5}$	$1.66\ 10^{-4}$	$4.27\ 10^{-5}$
FeII	$1.96\ 10^{-4}$	$6.76\ 10^{-5}$	$4.06\ 10^{-5}$	$6.76\ 10^{-5}$	$4.27\ 10^{-5}$
Ba	$1.43\ 10^{-9}$	$6.03\ 10^{-10}$	$2.21\ 10^{-8}$	$5.01\ 10^{-9}$	$1.23\ 10^{-10}$
Pt	$7.78\ 10^{-8}$	$1.78\ 10^{-8}$	$1.75\ 10^{-8}$		$5.75\ 10^{-11}$
Hg	$5.00\ 10^{-5}$	$4.47\ 10^{-7}$		$< 1.2610^{-8}$	$1.12\ 10^{-11}$

3.1. The primary (A) component

Titanium – 21 TiII lines of various multiplets, some of them in blends but in an acceptable fit, yield $N_{\rm Ti}/N_{\rm H} = 5.03(\pm 0.44)\,10^{-7}$, a value comparable with the KZZG value. This corresponds to a mild overabundance, enhanced by a factor of 5.

Chromium – 8 lines of CrII, Mult.No.44, give $N_{\rm Cr}/N_{\rm H} = 3.25(\pm 0.30)\,10^{-6}$. A mild to moderately strong overabundance, by a factor of 8, which is in good agreement with the KZZG value.

Manganese – four lines of MnI, Mult.No.2 (λ 403.0755, 403.3073, 403.449 nm) and No.5 (λ 404.1361 nm), and four lines of MnII, Mult.No.6 (λ 432.663 and λ 437.961 nm), No.7 (λ 425.92, 428.247 nm), yield $N_{\rm Mn}/N_{\rm H} = 2.74(\pm 0.31)\,10^{-6}$. Thus Mn is overabundant by a factor of 12, which amounts to only 1/3 of the value found in KZZG. A section of the spectrum with the three MnI Mult.No.2 lines is displayed in Fig.1.

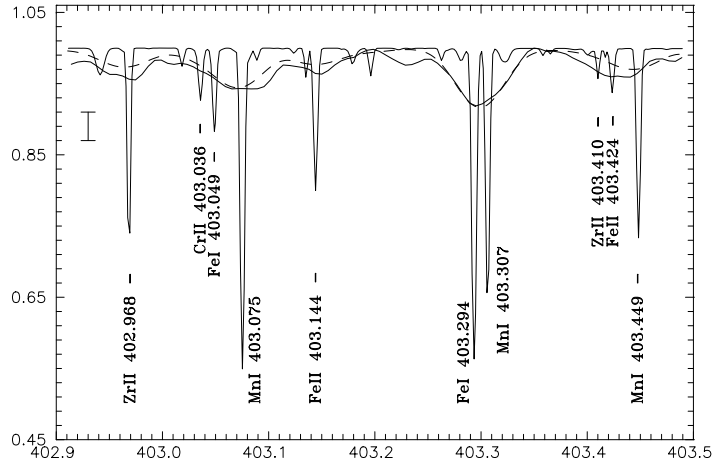

Figure 1. Computed and disentangled spectrum of the A component of AR Aur with three MnI Mult. No. 2 lines. Line identification is given for the synthetic spectrum (narrow spectral lines). Dashed line - synthetic spectrum after rotational and instrumental profile widening; full line - disentangled observed spectrum. The error bar for the observed spectrum is in the upper left corner of the figure. Abscissa - wavelength in nanometres, ordinate - relative intensity.

Iron – Four lines of FeI (λ 446.6551, 449.4564, 452.8613, 454.9463 nm) and 23 lines of FeII, mainly of multiplets 37 and 38, yield $N_{\rm Fe}/N_{\rm H} = 1.90(\pm 0.65)\,10^{-4}$ and $1.96(\pm 0.26)\,10^{-4}$, respectively. These values are higher by a factor of 2-3 than those published in KZZG, however, a scatter of single estimates ranges from 7 to $40\,10^{-5}$. Iron is in mild overabundance in the primary.

Barium – the BaII λ 455.4029 nm is blended by ZrII λ 455.396 nm. If Zr is estimated at $N_{\rm Zr}/N_{\rm H} = 6.0\,10^{-9}$, the abundance of barium is $N_{\rm Ba}/N_{\rm H} =$

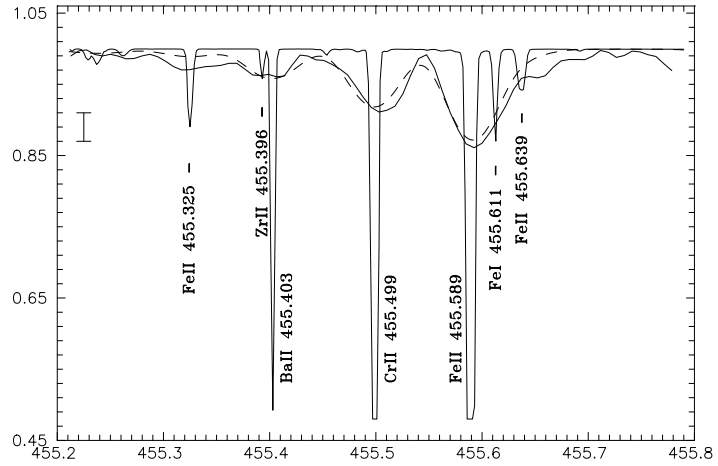

Figure 2. Section of the spectrum of the A component with the BaII 455.4029 nm line. The same symbolism as in Fig.1 was used.

$1.43\,10^{-9}$. This value also satisfies the fit at $\lambda\,413.1$ nm for Si $N_{\rm Si}/N_{\rm H} = 9.96\,10^{-5}$ (in a weak deficit also in accordance with $\lambda\,412.8059$ nm) and Mn $N_{\rm Mn}/N_{\rm H} = 2.74\,10^{-6}$. The section of the spectrum is shown in Fig.2.

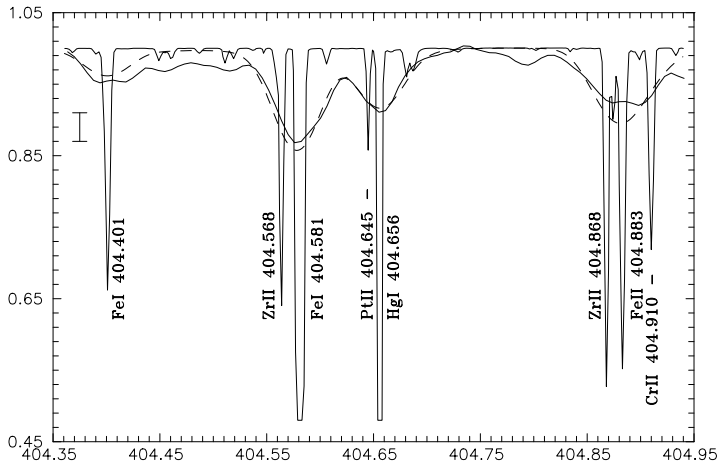

Figure 3. The strongest PtII line in the spectrum of A component and the HgI 404.6559 nm line. The same symbolism as in Fig.1 was used.

Platinum – three lines of PtII were used to estimate the abundance. Their $\log gf$-s were taken from Dworetsky & Vaughan (1984). The strongest line $\lambda\,404.645$ nm in the long-wave wing of FeI $\lambda\,404.5813$ nm is blended by HgI λ404.6559 nm, while CeII $\lambda\,404.6338$ nm with normal abundance does not contribute. The best fit was achieved for $N_{\rm Pt}/N_{\rm H} = 5.78\,10^{-8}$ with Fe abundance

$N_{Fe}/N_H = 7.8\,10^{-5}$ and Hg, derived from λ 398.3890 nm, $N_{Hg}/N_H = 5.0\,10^{-5}$. The fit is displayed in Fig.3.

The second strongest line λ 451.4170 nm occurs within a complex feature in which individual lines cannot be distinguished. If all the absorption were due to the PtII line, then platinum would have to be unreasonably overabundant, $N_{Pt}/N_H = 5.8\,10^{-6}$! The third line, λ 406.1660 nm, lies between two FeII lines, λ 406.1488 and 406.1782 nm. A relatively good fit can be achieved for the same Fe abundance as above and a slightly higher Pt, $N_{Pt}/N_H = 9.8\,10^{-8}$.

Mercury – the most remarkable feature of the binary spectrum is the HgII line λ 398.3890 nm. The abundance was derived from the λ 398.3890 nm line in spectra Nos 2 and 3 and the value was confirmed by HgI λ404.6559 nm. The coresponding fits are shown in Figs 3 and 4.

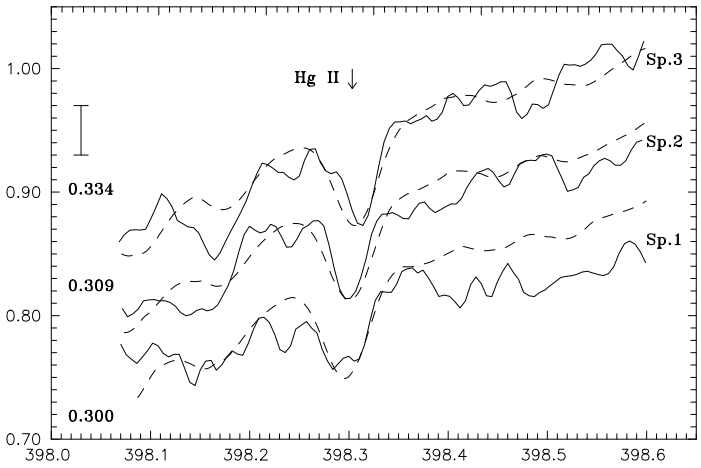

Figure 4. The HgII 398.389 nm line in orbital phases 0.300-0.334. Dashed line - synthetic compsite spectrum of the binary widened for rotation and instrumental profile. Full line - observed composite spectrum. Spectra No. 2 and 3 were shifted in the intesity scale.

Takeda et al.(1979) found that the line occured mainly near the orbital phase of the secondary minimum and Takada (1981) suggested that "the primary star has some inhomogeneities such as a cloud, a spot or a stratification". According to our observations the line is definitely present during the most of the orbital period, however, it seems to display a variable profile. In spectra Nos 2 and 3 (orbital phases 0.309, 0.334) the line is narrower and deeper than in the others. Another remarkable phenomenon can be observed: the observed profile is narrower than the one computed, widened by the values of $v \sin i$ and instrumental half-width satisfying all the other profiles studied. This is clearly demonstrated in Fig.4.

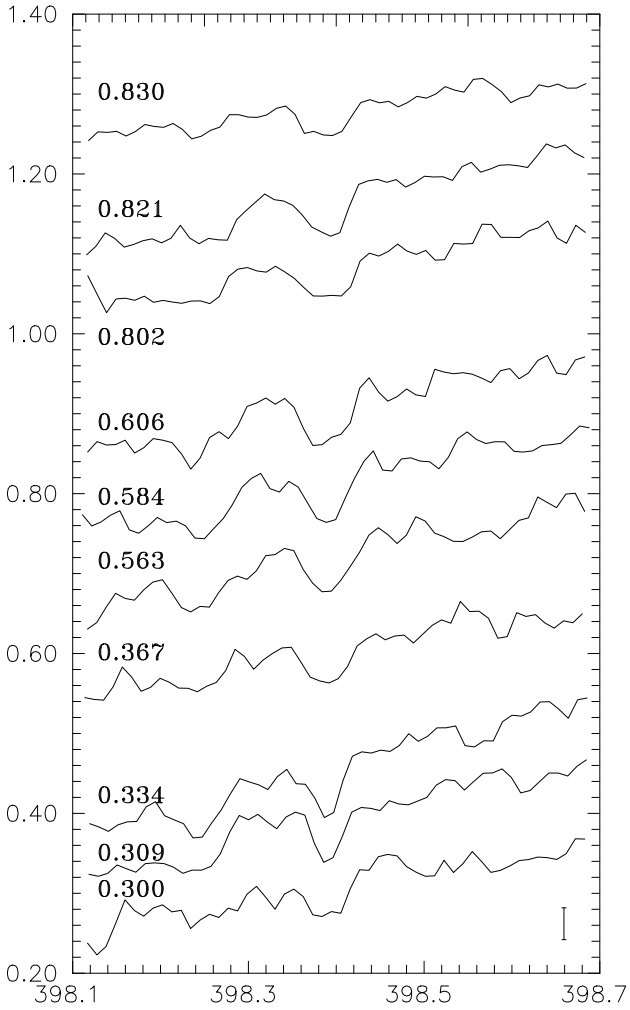

Figure 5. The varying profile of the HgII 398.389 nm line. Orbital phases are indicated in the left side, the error bar is in the lower right corner of the figure. Observed composite spectra are plotted. The ndividual spectra are shifted in ordinate, the radial velocity shifts of orbital motion are removed.

In some orbital phases the line has a complex profile as displayed in Fig.5,

which, however, cannot be studied from the point of view of the isotopic or spotty structure due to insufficient S/N and resolution of the spectrograms used.

Spectrum variability, the characteristic quality of CP2 stars caused by spotty distribution of elements over the star's surface, has not been definitely confirmed yet in HgMn-type stars. The above-mentioned facts, however, are evidence that mercury is distributed inhomogeneously over the surface of the primary.

3.2. The scondary (B) component

Titanium – twenty-two lines of TiII, Multiplet Nos 19, 20, 31, 41, 50, 51, 82, 105, 115 used led to the abundance value $N_{el}/N_H = 2.04(\pm 0.23)\,10^{-7}$. An acceptable fit was achieved for $N_{\rm Ti}/N_{\rm H}$ within the relatively narrow interval of $1 - 3\,10^{-7}$. The accepted value lies half way between the normal value and the KZZG value. The factor of two-fold overabundance indicates an almost normal content of the element.

Chromium – nine lines of Cr II, Multiplet Nos.31, and 44 give $N_{\rm Cr}/N_{\rm H} = 1.92(\pm 0.10)\,10^{-6}$ with the individual values within $1.4 - 2.2\,10^{-6}$. This value is practically identical with the KZZG value and indicates a less then five-fold overabundance.

Manganese – four lines of MnI, Mult.No.2 ($\lambda\,403.0755, 403.3073, 403.4490$ nm) and No.5 ($\lambda\,404.1361$ nm) and three lines of MnII, Mult.No.6 ($\lambda\,432.663$ nm) and No.7 ($\lambda\,425.920, 428.247$ nm) yield $N_{\rm Mn}/N_{\rm H} = 1.21(\pm 0.15)\,10^{-6}$ in good mutual agreement, as well as in agreement with the KZZG value of $1.58\,10^{-6}$. Relatively to the normal value, $2.24\,10^{-7}$ this indicates a six-fold overabundance. The fit of MnII, Mult.No.7, is diplayed in Fig.6.

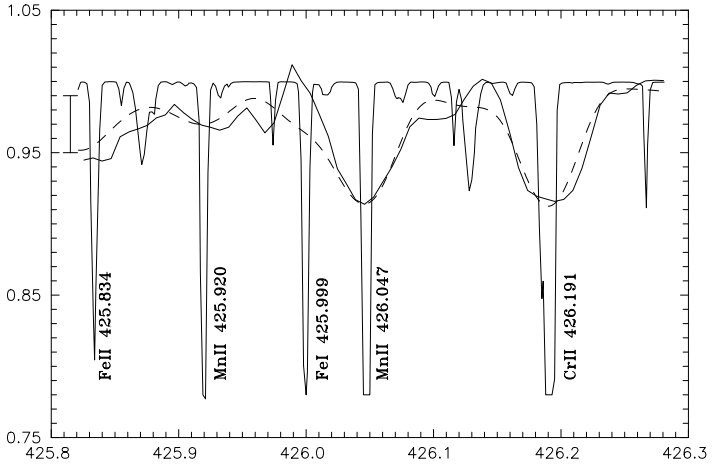

Figure 6. Two MnII lines in the spectrum of B component. Symbolism of Fig.1 was used.

Iron – eleven FeI lines of Mult.Nos 41, 42, 43, 152, 522, 693 yield $N_{\rm Fe}/N_{\rm H} = 6.25(\pm 0.50)\,10^{-5}$, whereas twelve FeII lines of Mult.Nos 37, 38 yield $N_{\rm Fe}/N_{\rm H} = 4.06(\pm 0.74)\,10^{-5}$, a value less than the former. A similar tendency in the FeI/FeII ratio, though to a far larger extent, was also obtained in KZZG. Taking into account the *normal* value, $4.27\,10^{-5}$, the abundance of iron, according to this analysis, is normal and the difference between these two values of abundances is insignificant.

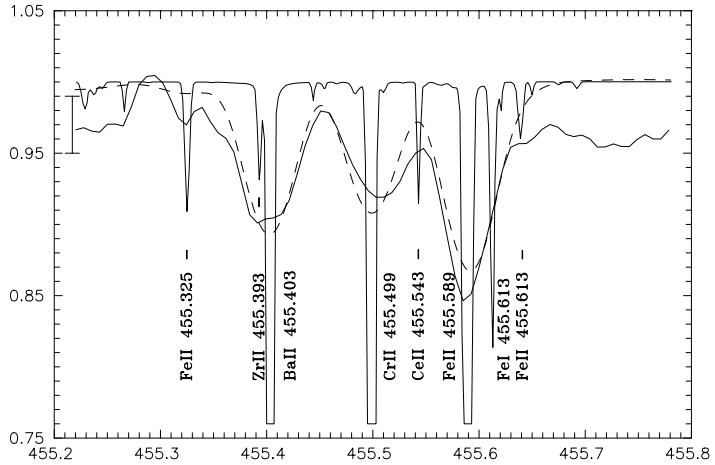

Figure 7. The BaII 455.4029 nm line in the spectrum of B component. Symbolism of Fig. 1 was used.

Barium – one line of BaII $\lambda\,455.4029$ nm could be used for abundance determination. Possible blending with CrI $\lambda\,455.395$ nm and ZrII $\lambda\,455.396$ nm is insignificant. For the Cr abundance derived above, the CrI line contribution amounts to less than 1% of the barium line equivalent width. The ZrII line contribution, assuming a 20-fold overabundance of the element in accordance with the KZZG, amounts to less than 5% of the overall equivalent width of the feature. Moreover, the above mentioned overabundance of Zr seems to be an upper limit as our estimate based on the ZrII line at $\lambda\,395.8230$ nm suggests zirconium is rather normal. To check the sensitivity of the line to temperature and gravity changes, we also computed the synthetic spectrum for atmosphere models $T_{\rm eff} = 10\,350{\rm K}, \log g = 4.1$ and 4.3 and $T_{\rm eff} = 10\,250$ and $10\,450{\rm K}, \log g = 4.2$. For $T_{\rm eff} = 10\,350{\rm K}$ the change of $\log g \pm 0.1$, as well as for $\log g = 4.2$ the change of $T_{\rm eff} \pm 100\,{\rm K}$ results in a central depth variation of the barium line by 0.5% which is well under our S/N ≈ 50 (2%). The second BaII line at $\lambda\,413.0645$ nm is an ingredient of the strong SiII line $\lambda\,413.0894$ nm. Another blending line is CeII $\lambda\,413.0705$ nm. Cerium lines usually occur in blends with other lines and a dispersion of its convenient abundance well exceeds 1.5 dex which makes any estimation of Ce abundance doubtful. A good fit of the $\lambda\,413.1$ nm feature can be achieved for cerium overabundant by a factor of 300 ($7.3\,10^{-9}$), manganese

by a factor of 4 ($N_{Ce}/N_H = 9.2\,10^{-7}$) and silicon deficient by a factor of 2 ($N_{Si}/N_H = 7.52\,10^{-5}$). Thus barium would be overabundant only by a factor of 8, remarkably lower than that derived from the λ 455.4029 nm line. The sections concerned are displayed in Figs 7 and 8. The third BaII line, λ 416.600 nm, is not present in the spectra of the secondary component.

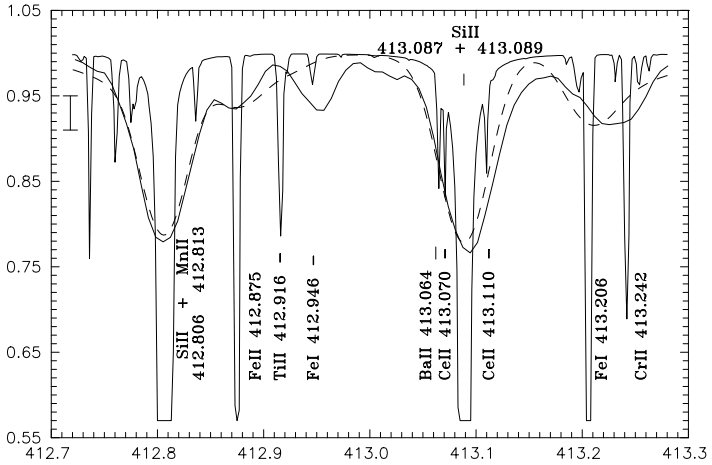

Figure 8. The BaII 413.0645 nm line in the left wing of the SiII blend. The same symbolism as in Fig.1 was used.

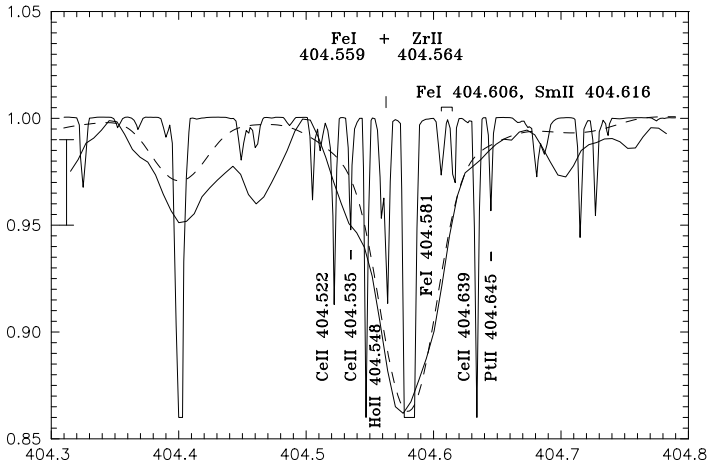

Figure 9. The PtII 404.645 nm line contribution to the blend of lines at 404.6 nm of the B component. The same symbolism was used as in Fig. 1.

Platinum – one line of PtII, λ 404.645 nm, is identified in the wing of the FeI λ 404.5813 nm. Other lines which could blend with the PtII one are CeII λ 404.6338 nm and HgI λ 404.6559 nm. While the CeII line helps to fit the

section of the FeI line profile, no additional line at the long-wave side of the PtII is needed as displayed on Fig.9. Indeed, for an overabundance of mercury by a factor of 4 dex, the equivalent width of this line is 0.13 pm, whereas the equivalent width of HgII λ 398.8389 nm is 1.16 pm, a value which is at the threshold of detectability in our spectra.

Even in the case of the upper limit, the contribution of HgI λ 404.6559 nm could not be practically resolved. The next strongest line of PtII could be identified at λ 451.417 nm. However, shortward of this vawelength in the observed spectrum occurs a relatively wide absorption feature, which could not be resolved into individual lines. At its centre lies MnII λ 451.3686 nm which, of course, cannot fulfill the whole obseved feature with any realistic abundance.

4. Conclusions

We have determined the abundances of chosen chemical elements in the components of the SB2 binary AR Aur using the new method and the KOREL code for disentangling composite spectra. The method made it possible to avoid the main inconveniences arising from mutual blending of spectral lines originating in the individual binary components. For two models of stellar atmospheres having close $T_{\rm eff}$ and $\log g$ values we have confirmed different chemical peculiarities of the binary components. For the primary, the abundances of the iron peak elements agree with the characteristics of an HgMn-star given by Dworetsky (1994) as well as by Hubrig & Mathys (1994) for manganese and mercury.

The mercury HgII λ398.389 nm line belonging to the primary is the most remarkable feature of the binary spectrum. It seems to be variable over the orbital phase, its profile shows a complex structure, however, such an investigation needs better S/N and resolution spectrograms. In two spectra it is narrower than corresponds to rotational and instrumental broadening. Our finding confirms the above mentioned suggestion of Takada (1981) as well as comply with the Hubrig & Mathys (1994) statement, that on HgMn stars mercury is concentrated around equator.

The majority of spectral lines in the secondary component are blended mainly with rare elements lines most frequently by cerium lines. Their analysis, of course, will need a more detailed study.

Acknowledgements. The authors appreciate the participation of the late Professor W. Wehlau in the observations. VLK thanks the Institute of Astronomy, Cambridge, England, where the initial reduction of the spectra was performed. Our thanks belong to Dr. P. Hadrava who provided us with his code KOREL and to Dr. Z. Mikulášek who kindly read the manuscript and made valuable comments.

The work was supported by Grant VEGA 4175/97.

References

Dworetsky, M.M.: 1993, *Publ. Astron. Soc. Pac., Conference Series* **44**, 1
Dworetsky, M.M., Vaughan, Jr.A.H.: 1973, *Astrophys. J.* **181**, 811
Hadrava, P.: 1995, *Astron. Astrophys., Suppl. Ser.* **114**, 393
Hadrava, P.: 1996, *KOREL - User's guide*, preprint
Hubený, I.: 1987, *Sci. Tech. Rep. Astron. Inst. Czechoslov. Acad. Sci.* **40**
Hubrig, S., Mathys, G.: 1994, in *Astronomy Posters Abstracts, XXIInd GA of the IAU*, ed.: H.van Woerden, Twin Press, Sliedrecht, The Netherlands, 235
Chochol, D., Juza, K., Mayer, P., Zverko, J., Žižňovský, J.: 1988, *Bull. Astron. Inst. Czechosl.* **39**, 69
Khokhlova, V.L., Zverko, J., Žižňovský, J., Griffin, R.E.M.: 1995, *Astron. Lett.* **21**, 818
Kurucz, R.L.: 1993, *Publ. Astron. Soc. Pac., Conference Series* **44**, 87
Nordström, B., Johansen, K.T.: 1994, *Astron. Astrophys.* **282**, 787
Romanyuk, I.I.: 1996, *private comm.*
Takada, M..: 1981, *private comm.*
Takeda, Y., Takada, M., Kitamura, M.: 1979, *Publ. Astron. Soc. Japan* **31**, 821
Wolff, S.C., Preston, G.W.: 1978, *Astrophys. J., Suppl. Ser.* **37**, 371
Wolff, R.J., Wolff, S.C.: 1976, *Astron. J.* **203**, 171
Zboril, M.: 1989, *private comm.*